Random Geometric Graphs

P. Van Mieghem*

Delft University of Technology
21 October 2026

Abstract

After a brief overview of Random Geometric Graphs and their corresponding distribution for the degree and number of links, we concentrate on Hard Random Geometric Graphs, for which the link density can be computed analytically. Both Euclidean and hyperbolic embeddings on nodes are explained.

1 Definition of Random Geometric Graphs (RGG)

Erdős-Rényi random graphs are created from a set $\mathcal{N}$ of N nodes, where each pair of nodes is connected by a link with probability p, independently of the existence of any other link [1, 2].

By placing the nodes in a d-dimensional metric space $\mathcal{S}$, where a distance function is defined, geometry is added to a graph: each node has a coordinate or position in the metric space $\mathcal{S}$ and the distance between nodes can be computed. The position r_i of each node i in the metric space $\mathcal{S}$ can be either deterministic or stochastic. In remarkably few networks[1], the nodal positions are precisely known; thus deterministic. However, in most networks, the precise nodal positions are not known publicly or only a (small) set of nodal positions is known. In such cases, the positions are modelled stochastically, where the probabilistic setting introduces randomness, that reflects our uncertainty about the precise nodal positions in a partially observed network.

If the node i at position r_i and the node j at position r_j in the metric space $\mathcal{S}$ are connected by a link with probability $p_{ij} = f(|r_i - r_j|)$, where $f(r)$ is a non-negative real function of the distance r, then we talk about a *random geometric graph* (RGG) [3]. If $f(r) = 1_{r<r_0}$, where 1_x is the indicator function[2], then all nodes at distance smaller than r_0 are connected. Although link creation is then deterministic, such type is called a *hard random geometric graph* (HRGG), where random refers to the stochastic position of the nodes. The idea of relating the probability of a link between nodes i and j to some function $f(r)$ of the distance $r = |r_i - r_j|$ between those nodes stems from realistic networks. The farther two nodes lie separated, the less the need for a direct link between them as well

*Faculty of Electrical Engineering, Mathematics and Computer Science, P.O Box 5031, 2600 GA Delft, The Netherlands; *email*: P.F.A.VanMieghem@tudelft.nl

[1] Only transportation networks are publicly available, such as road networks where cross-sections can be represented as nodes, while the roads or streets are the links. Via route planners (e.g. Google maps), a route from one place with GPS coordinate to another can be generated.

[2] The indicator function $1_x = 1$, if the condition or event x is true, else $1_x = 0$.

as the smaller the possibility to connect them by a link in infrastructural networks (e.g. by a wireless, optical, electricity link, by a direct road in a transport network, by a pipe in a utility network, etc.).

If positions are stochastic, then the link existence is doubly stochastic and depends both on the distance function $f(r)$ and on the random placement of nodes described by a joint probability distribution $\Pr[r_1 \leq x_1, \cdots, r_N \leq x_N]$.

In the sequel, we summarize the theory in [4] and [3].

2 Number of links and degree in a RGG

A link l_{ij} in a RGG between node i and node j is a Bernoulli random variable [5] that takes the value $l_{ij} = 1$, meaning that the link exists, with probability p_{ij} or $l_{ij} = 0$ (no link) with probability $1 - p_{ij}$. The attractive feature of a Bernoulli random variable is that the expectation $E[l_{ij}] = \Pr[l_{ij} = 1]$. In other words, the difficult probability operator $\Pr[.]$ can be replaced by the linear expectation operator $E[.]$ and the powerful theory of the probability generating function $\varphi_X(z) = E\left[z^X\right] = \sum_{k=0}^{\infty} \Pr[X = k] z^k$ of a discrete random variable X is applicable [5, Sec. 2.2.2]. In particular, the probability generating function (pgf) is a Taylor series[3] around $z_0 = 0$ with Taylor coefficient equal to

$$\Pr[X = k] = \frac{1}{k!} \left. \frac{d^k \varphi_X(z)}{dz^k} \right|_{z=0} \tag{1}$$

$$= \frac{1}{2\pi i} \int_{C(0)} \frac{\varphi_X(z)}{z^{k+1}} dz \tag{2}$$

where the complex integral (2) along a closed contour $C(0)$ around the origin $z_0 = 0$ follows from Cauchy's powerful integral theorem [6]. In summary, once the pgf $\varphi_X(z)$ of the random variable X is known, the corresponding probability $\Pr[X = k]$ can always be computed.

2.1 Expectation of the number of links

The number of links $L[\mathcal{R}]$ in a RGG, specified by the N nodal positions $\mathcal{R} = \{r_1, r_2, \cdots, r_N\}$ in a metric space $\mathcal{S}$, is the sum over $\binom{N}{2}$, i.e all possible links, Bernoulli random variables

$$L[\mathcal{R}] = \sum_{i=1}^{N} \sum_{j=i+1}^{N} l_{ij}$$

with expectation, due to linearity $E\left[\sum_{i=1}^{N} \sum_{j=i+1}^{N} l_{ij}\right] = \sum_{i=1}^{N} \sum_{j=i+1}^{N} E[l_{ij}]$,

$$E[L[\mathcal{R}]] = \sum_{i=1}^{N} \sum_{j=i+1}^{N} p_{ij} = \sum_{i=1}^{N} \sum_{j=i+1}^{N} f(|r_i - r_j|) \tag{3}$$

where $f(r)$ is a real, non-negative function that defines links between nodes at distance r in a RGG.

[3] A function $f(z)$, that is analytic in a region S of the complex plane, can be expanded in a Taylor series $f(z) = \sum_{k=0}^{\infty} f_k(z_0)(z - z_0)^k$ around a point $z_0 \in S$. That Taylor series converges for all $|z - z_0| < R$, where R is the radius of the largest circle, with center at z_0, that lies inside the region S.

2.2 Probability that the number of links equals k

Since the distance[4] in any metric space $\mathcal{S}$ obeys the triangle inequality, $|r_i - r_k| \leq |r_i - r_j| + |r_j - r_k|$, the introduction of geometry destroys the independence (or almost independence) of links in the Erdős-Rényi random graph. Indeed, if link l_{ij} and link l_{ik} exist, which means that node i, node j and node k are close to each other, then the existence of link l_{jk} has higher probability to exist than based on independence alone without nodal positions. Hence, links in a RGG are generally not independent, but in some cases, the assumption of independence might be a reasonable approximation. If independence cannot be assumed, then the computation of graph metrics, such as degree, number links, number of triangles, etc. becomes challenging.

If we assume that each link l_{ij} is independent of any other link in a RGG, then the number of links $L[\mathcal{R}]$ is a sum of independent Bernoulli random variable with probability generating function (pgf)

$$E\left[z^{L[\mathcal{R}]}\right] = E\left[z^{\sum_{i=1}^{N}\sum_{j=i+1}^{N} l_{ij}}\right] = \prod_{i=1}^{N}\prod_{j=i+1}^{N} E\left[z^{l_{ij}}\right]$$

The pgf is $E\left[z^{l_{ij}}\right] = z^0 \Pr\left[l_{ij}=0\right] + z^1 \Pr\left[l_{ij}=1\right] = (1-p_{ij}) + p_{ij}z = 1 + p_{ij}\left(z-1\right)$ so that

$$E\left[z^{L[\mathcal{R}]}\right] = \prod_{i=1}^{N}\prod_{j=i+1}^{N} \left(1 + p_{ij}\left(z-1\right)\right)$$

After out-multiplying the product, a polynomial (thus finite Taylor series) in $(z-1)$ is found, from which $\Pr\left[L[\mathcal{R}]=k\right]$ can be computed via (1) or (2).

If all links have equal probability $p_{ij} = p$, as in Erdős-Rényi random graphs, then $E\left[z^{L[\mathcal{R}]}\right] = (1-p+pz)^{\binom{N}{2}}$ and Newton's binomium results in

$$\Pr\left[L[\mathcal{R}]=k\right] = \binom{\binom{N}{2}}{k} p^k \left(1-p\right)^{\binom{N}{2}-k}$$

Hence, the probability that there are k links in a RGG, where each link has the same probability p, is a binomial distributed with parameters p and $\binom{N}{2}$, which is the maximum possible number of links in any graph. In particular, only the complete graph has $L_{\max} = \binom{N}{2}$ links.

2.3 Probability that the degree of a random node equals k

Likewise, the degree of a node i equals $D_{RGG;i}[\mathcal{R}] = \sum_{j=1;j\neq i}^{N} l_{ij}$. The assumption of independence of the links again produces a sum of $N-1$ independent Bernoulli random variables with pgf

$$\begin{aligned}\varphi_{D_{RGG;i}}(z) = E\left[z^{D_{RGG;i}[\mathcal{R}]}\right] = E\left[z^{\sum_{j=1;j\neq i}^{N} l_{ij}}\right] &= \prod_{j=1;j\neq i}^{N} E\left[z^{l_{ij}}\right] \\ &= \prod_{j=1;j\neq i}^{N} \left(1 + p_{ij}\left(z-1\right)\right)\end{aligned}$$

[4] We use the notation $|r_i - r_j|$ for distance, although $\|r_i - r_j\|$ is more appropriate in higher dimensions, where r_i and r_j are vectors and $\|.\|$ is a matrix or vector norm [7, Sec. 9.2].

If all links have equal probability $p_{ij} = p$, so that $D_{RGG;i}[\mathcal{R}] = D_{RGG}[\mathcal{R}]$, then we find that

$$\Pr\left[D_{RGG}[\mathcal{R}] = k\right] = \binom{N-1}{k} p^k \left(1-p\right)^{N-1-k}$$

Hence, if the link probability $p_{ij} = p$ and links are nearly independent, then the degree $D_{RGG}[\mathcal{R}]$ of a random node in a RGG is a binomial random variable with parameters p and $N-1$ and $\mathcal{R}$. Clearly, if $p = 1$, then randomness disappears and the RGG becomes the complete graph K_N.

2.4 General analysis of the link density in a RGG

If nodes are randomly placed at positions $\mathcal{R}$, then the expectation $E\left[L[\mathcal{R}]\right]$ in (3) is a random variable, else $E\left[L[\mathcal{R}]\right]$ is positive real number. The average over all possible configurations $\mathcal{R}$ of nodes in a chosen finite volume v of the d-dimensional space $\mathcal{S}$ generated by the link connection function $f(.)$ produces the average number of links

$$L_{av} = \int_v E\left[L[\mathcal{R}]\right] \Pr[\mathcal{R}] \; d\mathcal{R}$$

where

$$\Pr[\mathcal{R}] = \frac{\partial^N \Pr\left[r_1 \leq x_1, r_2 \leq x_2, \ldots, r_N \leq x_N\right]}{\partial x_1 \partial x_2 \ldots \partial x_N} = g_{\{r_1, r_2, \ldots, r_N\}}\left(x_1, x_2, \ldots, x_N\right)$$

is the joint probability density function (pdf) of the positions $\mathcal{R}$ of the set of nodes, resulting with (3) in

$$L_{av} = \int_v dx_1 dx_2 \ldots dx_N g_{\{r_1, r_2, \ldots, r_N\}}\left(x_1, x_2, \ldots, x_N\right) \sum_{i=1}^{N} \sum_{j=i+1}^{N} f\left(|x_i - x_j|\right) \tag{4}$$

Thus, r_j is a d-dimensional random variable and x_j is a deterministic d-dimensional vector with coordinates $x_j = \left((x_j)_1, (x_j)_2, \ldots, (x_j)_D\right)$.

We can proceed further if we assume independence in the nodal positions,

$$\Pr\left[r_1 \leq x_1, r_2 \leq x_2, \ldots, r_N \leq x_N\right] = \prod_{k=1}^{N} \Pr\left[r_k \leq x_k\right]$$

with corresponding joint pdf $g_{\{r_1, r_2, \ldots, r_N\}}\left(x_1, x_2, \ldots, x_N\right) = \prod_{k=1}^{N} g_{r_k}\left(x_k\right)$ consisting, by independence, in a product of N single pdfs $g_{r_k}\left(x\right) = \frac{d \Pr[r_k \leq x]}{dx}$. Then, the average number of links in (4) simplifies to

$$\begin{aligned} L_{av} &= \int_v \prod_{k=1}^{N} g_{r_k}\left(x_k\right) dx_k \sum_{i=1}^{N} \sum_{j=i+1}^{N} f\left(|x_i - x_j|\right) \\ &= \sum_{i=1}^{N} \sum_{j=i+1}^{N} \int_v dx_i \int_v dx_j g_{r_i}\left(x_i\right) g_{r_j}\left(x_j\right) f\left(|x_i - x_j|\right) \end{aligned}$$

Further, we assume that each node is placed in the d-dimensional space $\mathcal{S}$ in a similar or homogeneous way, so that the distributions of $\Pr\left[r_i \leq x\right] = \Pr\left[r_j \leq x\right]$ are the same and equal to $\Pr\left[r \leq x\right]$. The average number of links formula then reduces to

$$\begin{aligned} L_{av} &= \sum_{i=1}^{N} \sum_{j=i+1}^{N} \int_v dx \int_v dy \; g_r\left(x\right) g_r\left(y\right) f\left(|x - y|\right) \\ &= \binom{N}{2} \int_v dx \int_v dy \; g_r\left(x\right) g_r\left(y\right) f\left(|x - y|\right) \end{aligned}$$

The corresponding link density $p = \frac{L_{av}}{L_{\max}}$, where the maximum possible number of links $L_{\max} = \binom{N}{2} = \frac{N(N-1)}{2}$, for a set of nodes with i.i.d. placement strategy is

$$p = \frac{L_{av}}{L_{\max}} = \int_v dx \int_v dy \; g_r(x) \, g_r(y) \, f(|x-y|) \tag{5}$$

A final simplification is the assumption of *uniform* placement of the nodes in a space $\mathcal{S}$ with volume v, in which case $g_r(x) = \frac{1}{v}$. We then arrive at the link density of a RGG with i.i.d. uniformly placed nodes in a volume v for any link connection function $f(r)$,

$$p = \frac{L_{av}}{L_{max}} = \int_v \frac{dx}{v} \int_v \frac{dy}{v} \; f(|x-y|) \tag{6}$$

When the nodes are placed uniformly at random inside a d-dimensional rectangular hyperprism in the Euclidean space with edge lengths $Z_1, Z_2, \cdots, Z_d$ and volume $v_d = \prod_{k=1}^{d} Z_k$, so that $g_r(x) = \frac{1}{v_d}$, the integral in (6) can be analytically evaluated, for which we refer to [3].

2.5 Formula (6) of the link density in a RGG

We observe that the link density (6) is a *purely geometric property* and does not depend on the number N of nodes, in contrast to the average degree. Indeed, the basic law $d_{av} = \frac{2L_{av}}{N} = p(N-1)$ of the nodal degree in any graph [7] maps the link density p to the average degree d_{av} or expectation $E[D] = \frac{2L_{av}}{N}$ of the random degree D.

The importance and practical use of the link density formula (6) for an RGG (under the stated assumptions in Section 2.4 of i.i.d. uniform placement) lies in at least two aspects.

First, only if links in an RGG are almost independent from each other, the connectivity in a RGG with N nodes and link density p in (6) is well approximated by the theory of Erdős-Rényi random graph $G_p(N)$. For large N, the Erdős-Rényi random graph $G_p(N)$ is connected [5, Sec. 17.5.3], [1, 2] almost surely if the link density $p > p_c$, where the critical threshold $p_c = \frac{\log N}{N} + O\left(\frac{1}{N}\right)$. Hence, only if link independence is a good approximation, then a sufficiently large RGG with link density p in (6) is almost surely connected if $p > \frac{\log N}{N}$ and disconnected if $p < \frac{\log N}{N}$ (see also [4, Sec. 4.2; Appendix C]). Generally, the link dependence in a RRG may cause a lower link density p at which disconnectivity of the RGG occurs.

Second, when both the topologies of the Erdős-Rényi random graph $G_p(N)$ and the Waxman graph on N nodes, defined by the link connection function $f(r) = e^{-ar}$, possess exponentially or uniformly distributed link weights, the probability distribution of the hopcount of the shortest path between two arbitrary nodes is almost identical [8], [5, Chapt. 16] in both graphs for the same link density p, related via (6), even for a relatively small number N of nodes. In unweighted RGGs or in RGGs with unit link weights, however, the shortest paths can deviate much [9] in different RGGs.

3 Link density of the RGG in a two-dimensional square

In this section, we confine ourselves to a $d = 2$ dimensional square $\square$ with $Z_1 = Z_2 = Z$ in the Euclidean space, where the link density (6) reduces to

$$p_{\square} = \frac{1}{Z^4} \int_0^Z dx_1 \int_0^Z dx_2 \int_0^Z dy_1 \int_0^Z dy_2 f\left(\sqrt{(x_1-x_2)^2 + (y_1-y_2)^2}\right)$$

We show in [4, Appendix A] that this 4-dimensional integral can be reduced to a single integral

$$p_{\square} = \int_0^{Z\sqrt{2}} f(r) f_{\mathcal{D}}(r) dr \tag{7}$$

where the probability density function $f_{\mathcal{D}}(r)$ of the distance[5] $\mathcal{D}$ between two arbitrary points in the square with size Z equals

$$f_{\mathcal{D}}(r) = \begin{cases} \frac{1}{Z^4}\left(2\pi r Z^2 - 8r^2 Z + 2r^3\right) & \text{for } 0 \le r \le Z \\ \frac{1}{Z^4}\left(Z^2 r(2\pi - 4) + 8Zr\sqrt{r^2 - Z^2} - 8Z^2 r \arccos\left(\frac{Z}{r}\right) - 2r^3\right) & \text{for } Z \le r \le Z\sqrt{2} \end{cases} \tag{8}$$

Since the pdf $f_{\mathcal{D}}(r)$ in (8) of the HRGG is one of the very few exact results, a further exploration is recommended.

The probability distribution function $F_{\mathcal{D}}(r) = \Pr[\mathcal{D} \le r]$ of the distance $\mathcal{D}$ between two random points in the square with size Z, which is equal to $F_{\mathcal{D}}(r) = \int_0^r f_{\mathcal{D}}(r) dr$, shows that $\int_0^{Z\sqrt{2}} f_{\mathcal{D}}(r) dr = 1$, because $\mathcal{D} \le Z\sqrt{2}$ and the longest possible distance $Z\sqrt{2}$ is the length of the diagonal of the square. We notice that $\lim_{r \uparrow Z} f_{\mathcal{D}}(r) = \frac{2}{Z}(\pi - 3)$ and $\lim_{r \downarrow Z} f_{\mathcal{D}}(r) = \frac{2}{Z}((\pi - 2) - 4\arccos(1) - 1) = \frac{2}{Z}(\pi - 3)$. Thus, $f_{\mathcal{D}}(r)$ is continuous[6] at $r = Z$. Hence, the pdf $f_{\mathcal{D}}(r)$ is continuous for all real $0 \le r \le Z\sqrt{2}$.

Applying the Integral Mean Value Theorem[7] to (7), tells us that there exist a real value $\varphi \in \left[0, Z\sqrt{2}\right]$, such that

$$p_{\square} = \int_0^{Z\sqrt{2}} f(r) f_{\mathcal{D}}(r) dr = f(\varphi) \tag{10}$$

Since usually the continuous function $f(r)$ – which excludes $f(r) = 1_{\{r \le r_0\}}$ for a HRGG – is decreasing in r, such as e.g. $f(r) = e^{-ar^{\eta}}$ in [3] for positive real a and η, the maximum of $f(r)$ occurs at $f(0)$ and the minimum at $f\left(Z\sqrt{2}\right)$. Consequently, (10) is maximal at $p_{\square} = f(0)$, which must equal 1 if we wish that the RGG can construct all possible link densities. The minimum possible link density $p_{\square} = f\left(Z\sqrt{2}\right)$ should be ideally zero or, if connectivity of RGG is regarded as important, equal to some link density threshold p_c under which the graph is almost surely disconnected, such as $p_c \sim \frac{\log N}{N}$ for Erdős-Rényi graphs with sufficiently large N.

3.1 Link density of Hard RGG in a square

For a HRGG with $f(r) = 1_{\{r \le r_0\}}$, execution of (7) yields a link density

$$p_{\square;HRGG}(r_0) = \int_0^{r_0} f_{\mathcal{D}}(r) dr = \Pr[\mathcal{D} \le r_0] \tag{11}$$

The link density in a HRGG on a square $\square$ with size Z with link connection radius r_0 equals the probability that the random distance $\mathcal{D}$ between two uniformly at random placed nodes in the square

[5] The random variable of the distance is denoted by "round" $\mathcal{D}$, while the random variable of the degree by D.

[6] Probability theory only requires that the probability distribution function $F_X(x) = \Pr[X \le x]$ of a random variable X is continuous "at the right". Hence, $F_X(x)$ is not necessarily continuous and may possess jumps [5, p. 16]. Even if $F_X(x)$ is continuous, the pdf $f_X(x) = \frac{dF_X(x)}{dx}$ is not necessarily continuous.

[7] The Integral Mean Value Theorem [10, p. 322] states: For a real continuous function $g(x)$ on the interval $[\alpha, \beta]$ and a function $p(x)$, which is positive and integrable on the interval $[\alpha, \beta]$, there exists a real number $\varphi \in [\alpha, \beta]$ such that

$$\int_{\alpha}^{\beta} p(x) g(x) dx = g(\varphi) \int_{\alpha}^{\beta} p(x) dx \tag{9}$$

is smaller than the link connection radius r_0. Hence, the link density also equals the probability to have a link between any two nodes in HRGG.

If boundary effects can be ignored for sufficiently small link connection radius $r_0 << Z$, then nodes can be regarded as indistinguishable in the sense that each node sees a same surrounding (which does not apply for nodes close to the boundary or close to corners of the square). The indistinguishability between nodes and their nodal position independence then produce[8], to a good approximation, similarly as in an Erdős-Rényi random graph and as shown in Section 2, the binomial probability distribution $\Pr\left[D_{HRGG}=k\right] \simeq \binom{N-1}{k} p_{\square;HRGG}^{k}\left(r_0\right)\left(1-p_{\square;HRGG}\left(r_0\right)\right)^{N-1-k}$ of the degree D_{HRGG} of a node in HRGG with average degree

$$d_{av;HRGG} = E\left[D_{HRGG}\right] = \left(N-1\right) p_{\square;HRGG}\left(r_0\right) \tag{12}$$

After transforming (11) into the normalized length $u = \frac{r}{Z}$, the link density $p_{\square;HRGG}\left(r_0\right) = Z\int_0^{\frac{r_0}{Z}} f_{\mathcal{D}}\left(Zu\right) du$ expresses the pdf (8) as

$$Z f_{\mathcal{D}}\left(Zu\right) = \begin{cases} 2\left(\pi u - 4u^2 + u^3\right) & \text{for } 0 \leq u \leq 1 \\ 2\left(\left(\pi-2\right)u + 4u\sqrt{u^2-1} - 4u\arccos\left(\frac{1}{u}\right) - u^3\right) & \text{for } 1 \leq u \leq \sqrt{2} \end{cases} \tag{13}$$

We use the indefinite integrals with constants K_1 and K_2,

$$I_1\left(u\right) = \int \left(\pi u - 4u^2 + u^3\right) du = \frac{\pi}{2}u^2 - \frac{4}{3}u^3 + \frac{1}{4}u^4 + K_1$$

and[9]

$$\begin{aligned} I_2\left(u\right) &= \int \left(\left(\pi-2\right)u + 4u\sqrt{u^2-1} - 4u\arccos\left(\frac{1}{u}\right) - u^3\right) du \\ &= \frac{\pi-2}{2}u^2 + \frac{4}{3}\left(u^2-1\right)^{\frac{3}{2}} - 2u^2\arccos\left(\frac{1}{u}\right) + 2\sqrt{u^2-1} - \frac{1}{4}u^4 + K_2 \end{aligned}$$

Since $I_1\left(0\right) = \lim_{r_0\to 0}\frac{1}{2}\int_0^{r_0} f_{\mathcal{D}}\left(r\right) dr = 0$, it holds that $K_1 = 0$, so that $I_1\left(1\right) = \frac{\pi}{2} - \frac{13}{12}$. Further $I_2\left(1\right) = \frac{\pi}{2} - \frac{5}{4} + K_2$, combined with $I_1\left(1\right) = I_2\left(1\right)$ due to continuity, determines $K_2 = \frac{\pi}{2} - \frac{13}{12} - \frac{\pi}{2} + \frac{5}{4} = \frac{1}{6}$. Thus, if $r_0 \leq Z$, then the link density in a HRGG on a square with size Z is

$$p_{\square;HRGG}\left(r_0\right) = \frac{1}{2}\left(\frac{r_0}{Z}\right)^4 - \frac{8}{3}\left(\frac{r_0}{Z}\right)^3 + \pi\left(\frac{r_0}{Z}\right)^2 \tag{14}$$

[8] Since the nodes i and j are placed at position r_i and r_j independently and uniformly ad random over the square, their random distance equals $\mathcal{D}$. This holds for any pair of nodal positions. Hence, there are k links at node i if

$$\Pr\left[\left\{\cap_{j=1}^{k}\left|r_j - r_i\right| \leq r_0\right\} \cap \left\{\cap_{j=k+1}^{N}\left|r_j - r_i\right| > r_0\right\}\right] = \left(\Pr\left[\mathcal{D} \leq r_0\right]\right)^k \left(\Pr\left[\mathcal{D} > r_0\right]\right)^{N-k}$$

After taking all possible combinations of k nodes out of all N possible nodes, we arrive with (11) at (12).

[9] Partial integration leads to

$$\begin{aligned} \int u\arccos\left(\frac{1}{u}\right) du &= \frac{u^2}{2}\arccos\left(\frac{1}{u}\right) - \frac{1}{2}\int \frac{u}{\sqrt{u^2-1}} du \\ &= \frac{u^2}{2}\arccos\left(\frac{1}{u}\right) - \frac{1}{2}\sqrt{u^2-1} \end{aligned}$$

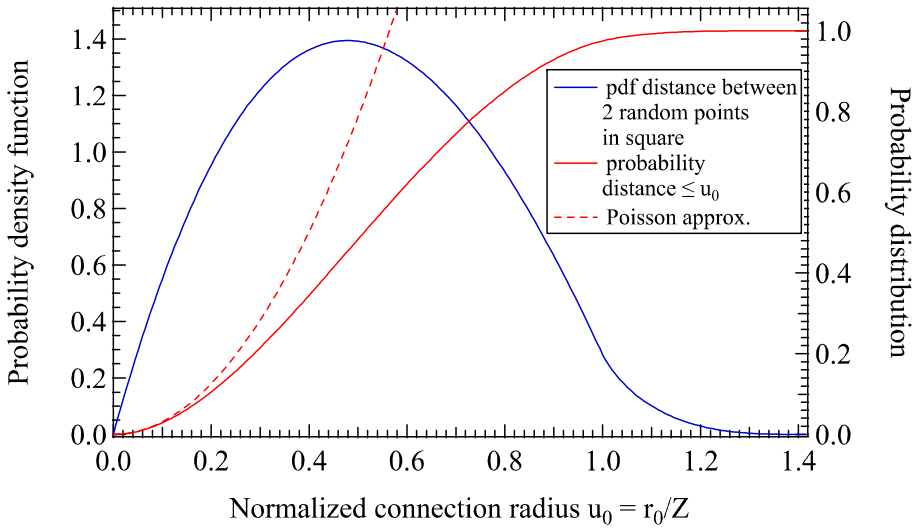


Figure 1: The pdf $f_{\mathcal{D}}(u_0)$ in (13) and its corresponding distribution $F_{\mathcal{D}}(u_0) = \Pr[\mathcal{D} \leq u_0]$, which also equals the link density (11) in a HRGG, versus normalized connection radius $u_0 = \frac{r_0}{Z}$. The Poisson approximation (red dotted line) equals $F_{\mathcal{D}}(u_0) \approx \pi u_0^2$ for small u_0.

If $Z \leq r_0 \leq Z\sqrt{2}$, then

$$p_{\square;HRGG}(r_0) = (\pi - 2)\left(\frac{r_0}{Z}\right)^2 + \frac{8}{3}\left(\left(\frac{r_0}{Z}\right)^2 - 1\right)^{3/2} - 4\left(\frac{r_0}{Z}\right)^2 \arccos\left(\frac{Z}{r_0}\right) + 4\sqrt{\left(\frac{r_0}{Z}\right)^2 - 1} - \frac{1}{2}\left(\frac{r_0}{Z}\right)^4 + \frac{1}{3} \tag{15}$$

We deduce from (14) that $p_{\square;HRGG}(Z) = \int_0^Z f_{\mathcal{D}}(r)\, dr = \pi - \frac{13}{6} = 0.974926$. Fig. 1 shows that, for $r_0 > Z$, we enter the tail region of the distribution. We verify from (15) that

$$p_{\square;HRGG}\left(Z\sqrt{2}\right) = 2(\pi - 2) + \frac{8}{3} - 8\arccos\left(\frac{1}{\sqrt{2}}\right) + 4 - \frac{1}{2}4 + \frac{1}{3} = 1$$

Indeed, $p_{\square;HRGG}\left(Z\sqrt{2}\right) = \Pr\left[\mathcal{D} \leq Z\sqrt{2}\right] = 1$ means that all nodes or points in the square with size Z lie inside any circle with a center inside the square and with radius $r_0 = Z\sqrt{2}$. The resulting RGG with $r_0 = Z\sqrt{2}$ is the complete graph.

The link density $p_{\square;HRGG}(r_0)$ in (11) is a differentiable, strictly increasing function of the connection radius r_0 that varies from $p_{\square;HRGG}(0) = 0$ to $p_{\square;HRGG}\left(Z\sqrt{2}\right) = 1$. In other words, by tuning the normalized connection radius $u_0 = \frac{r_0}{Z}$ in the interval $\left[0, \sqrt{2}\right]$, any link density between 0 and 1 can be achieved. Also, since the link density $p_{\square;HRGG}(r_0) = F_{\mathcal{D}}(r_0)$ in (11) is a probability distribution function and since the inverse function of a continuous probability distribution function always exists, the inverse function of $p = p_{\square;HRGG}(r_0)$ exists $r_0 = p^{-1}_{\square;HRGG}(p)$. The connection radius

$$r_0 = p^{-1}_{\square;HRGG}(p) \tag{16}$$

as a function of the link density p can be read from Fig. 1, but the inverse function $p^{-1}_{\square;HRGG}(x)$ is not analytically available. In other to construct a HRGG with link density p, the connection radius r_0 is key, which emphasizes the importance of the inverse function.

3.2 Asymptotics of HRGG for $N \to \infty$

The link density (6) and in particular (14) and (15) for the HRGG in a square with size Z does not depend upon the number of nodes N. On the other hand, if we require that the average degree $d_{av} = p\,(N-1)$ is kept constant when $N \to \infty$, then the connection radius (16) is

$$r_0 = p^{-1}_{\square;HRGG}\left(\frac{d_{av}}{N-1}\right)$$

To achieve a small link density $p = \frac{d_{av}}{N-1}$ for $N \to \infty$, the strictly increasing nature of (14) with r_0 implies a small connection radius r_0,

$$\begin{aligned} p_{\square;HRGG}\,(r_0) &= \pi\left(\frac{r_0}{Z}\right)^2\left(1 - \frac{8}{3\pi}\left(\frac{r_0}{Z}\right) + \frac{1}{2\pi}\left(\frac{r_0}{Z}\right)^2\right) \\ &= \pi\left(\frac{r_0}{Z}\right)^2\left(1 + O\,(r_0)\right) \end{aligned} \tag{17}$$

that leads[10], after inversion, ignoring the order term $O\,(r_0)$ in $1 + O\,(r_0)$ and noting the inequality $p_{\square;HRGG}\,(r_0) < \pi\left(\frac{r_0}{Z}\right)^2$ for small r_0, to

$$r_0 \approx Z\sqrt{\frac{1}{\pi}\frac{d_{av}}{N-1}} \tag{18}$$

In other words, if the number of nodes N grows unboundedly, the connection radius r_0 must decrease as $r_0 = O\left(\frac{1}{\sqrt{N}}\right)$ in order to produce a HRGG with average degree d_{av}. This scaling result (18) is known and follows elegantly from Poisson processes.

Connectivity, however, is a concern. Indeed, the ER-theory states that the link density $p > p_c$, where the critical link density threshold $p_c = \frac{\log N}{N} + O\left(\frac{1}{N}\right)$. If connectivity is required in very large HRGG, then the average degree $d_{av} = p\,(N-1)$ should scale or grow as $O\,(\log N)$. In other words, if d_{av} is kept constant while N increases, then the asymptotic RGG is almost surely disconnected.

3.2.1 Poisson approximation

The nodal density in the rectangle with length a and height b is $n = \frac{N}{ab}$. Node i has a link to node j if node j lies inside or on the boundary of a circle C_i with center at node i and radius r_0. The average number of nodes inside the disk C_i, that lies within the rectangle with sizes a and b, equals $E\,[D_{\mathrm{RGG;P}}] = n\pi r_0^2$, where $D_{\mathrm{RGG;P}}$ is the Poisson random degree of any node, not just node i, because each node within or on the boundary of the disk C_i is connected to node i and because the boundary of the rectangle is ignored.

Since the uniform and independent sprinkling of nodes in the rectangle is achieved by a Poisson point process with rate n, the degree distribution of a node in RGG follows from the Poisson distribution [5, Sec. 7.4]

$$\Pr\left[D_{\mathrm{RGG;P}} = k\right] \approx \frac{\left(n\pi r_0^2\right)^k}{k!}e^{-n\pi r_0^2}$$

approximately (because $\Pr\left[D_{\mathrm{RGG;P}} > N-1\right] \neq 0$ due to ignoring the boundary). If the number of nodes $N \to \infty$ and assuming that the link connection radius decreases as $r_0 = \rho_0 N^{-\beta}$, then the average

[10] Since $p_{\square;HRGG}\,(uZ) = \pi u^2 - \frac{8}{3}u^3 + \frac{1}{2}u^4$ is a polynomial of degree 4 in $u < 1$, its roots and thus the inversion $p^{-1}_{\square;HRGG}\,(uZ)$ can be computed analytically exactly. However, the result is not insightful and omitted.

degree is $E\left[D_{\mathrm{RGG;P}}\right] = \lim_{N\to\infty} \frac{\pi\rho_0^2}{ab} N^{1-2\beta}$, which is only positive, finite and equal to $E\left[D_{\mathrm{RGG;P}}\right] = \frac{\pi\rho_0^2}{ab}$ (which agrees with (18)), provided that we choose $\beta = \frac{1}{2}$. If both the number N of nodes and the link connection radius r_0 tend independently of each other to their limit ∞ and 0, respectively, then the average degree $E\left[D_{\mathrm{RGG;P}}\right]$ is not defined anymore.

Another advantage of the Poisson approximation is the extension to higher dimensions d. Since the volume[11] of a sphere in the d-dimensional Euclidean space with radius r_0 equals

$$v_{D\text{-sphere}}\left(r_0\right) = \frac{\pi^{\frac{d}{2}} r_0^d}{\Gamma\left(\frac{d}{2}+1\right)}$$

and the nodal density in a d-hyperprism with same edge length Z is $n_d = \frac{N}{Z^d}$, the expectation of the degree of d-HRGG, created by the d-Poisson point process and ignoring the boundary, is $E\left[D_{\text{D-RGG;P}}\right] \approx N \frac{\pi^{\frac{d}{2}}}{\Gamma\left(\frac{d}{2}+1\right)} \left(\frac{r_0}{Z}\right)^d$. The requirement that the average degree $E\left[D_{\text{D-RGG;P}}\right] = d_{av}$ should be finite and fixed, leads to

$$r_0 \approx Z \left(\frac{\Gamma\left(\frac{d}{2}+1\right)}{\pi^{\frac{d}{2}}} d_{av} \right)^{\frac{1}{d}} N^{-\frac{1}{d}}$$

illustrating the scaling law $r_0 = O\left(N^{-\frac{1}{d}}\right)$ in d dimensions if $N \to \infty$. The scaling law $r_0 = O\left(N^{-\frac{1}{d}}\right)$ illustrates that the link connection radius in a d-HRGG decreases slower with N if the dimension d increases.

4 Link density of the HRGG in a two-dimensional Poincaré disk

The Hard Random Hyperbolic Graph in hyperbolic geometry is very similar to its Euclidean counterpart, discussed in Section 3.1 and can also be computed exactly for the "hard" link connection function $f\left(r\right) = 1_{\{r \le r_0\}}$. The link density or average degree in a Hard Random Hyperbolic Graph (HRHG) has been computed exactly by Krioukov *et al.* [11]. The major technical complication lies in computing distances, line segments and areas in hyperbolic geometry. We refer to Appendix A for a brief introduction.

Similarly as for the Hard Random Geometric Graph (HRRG) in the Euclidean square, the Hard Random Hyperbolic Graph (HRHG) is constructed by sprinkling N nodes "uniformly at random in the Poincaré disk with radius R" and connecting nodes by a link if the distance between their positions in the Poincaré disk is closer than some given r_0. For simplicity, we choose a curvature $K = -\left|K\right| = -1$. If nodes are placed uniformly at random over an area A, then the probability density function $g_{(r,\theta)}\left(x\right) = \frac{d\Pr[z \le x]}{dx}$ of the position $z = (r,\theta)$ in polar coordinates of a random node is $g_{(r,\theta)}\left(x\right) = \frac{1}{A}$ and (33) would indicate that

$$g_{(r,\theta)}\left(x\right) = \frac{1}{2\pi\left(\cosh\left(R\right)-1\right)}$$

However, Krioukov *et al.* [11] choose a uniformly at random distribution only over the angular direction θ, where the radial coordinate r is variable. Thus, the nodes with position $z = (r,\theta)$ lying in an

[11] The volume of an ellipsoid $\mathcal{E}$ in d dimensions with semi-axis lenghts $\alpha_1, \alpha_2, \ldots . \alpha_d$ equals $v_{\mathcal{E}} = \frac{\pi^{\frac{d}{2}}}{\Gamma\left(\frac{d}{2}+1\right)} \prod_{j=1}^{d} \alpha_j$.

infinitesimal area $dS_{\mathcal{H}} = \sinh(r)\, dr d\theta$ in (31) are uniformly distribution over the angles $\theta \in [0, 2\pi]$,

$$\frac{dS_{\mathcal{H}}}{A_{\text{disk}}} = \frac{\sinh(r)\, dr d\theta}{2\pi(\cosh(R) - 1)}$$

and

$$\Pr[x \leq z \leq x + dx] = \int_0^{2\pi} \frac{\sinh(r)\, dr d\theta}{2\pi(\cosh(R) - 1)} = \frac{\sinh(x)\, dx}{\cosh(R) - 1}$$

Since $\Pr[x \leq z \leq x + dx] = \frac{d\Pr[z \leq x]}{dx} dx$, the corresponding probability density function $g_{(r,\theta)}(x) = \frac{d\Pr[z \leq x]}{dx}$ of the position of a node at radial coordinate $r = x$ is

$$g_{(r,\theta)}(x) = \frac{\sinh(x)}{\cosh(R) - 1} \tag{19}$$

For large R, we approximate as $g_{(r,\theta)}(x) = \frac{e^x - e^{-x}}{e^R + e^{-R} - 1} \approx e^{x-R}$. In contrast to the Euclidean HRRG, the nodal density is chosen in [11] to dependent on the distance $r = x$ to the origin in the hyperbolic Poincaré disk.

Next, nodes are connected if their distance lies within a connection radius r_0, which Krioukov *et al.* [11] choose equal to the radius R of hyperbolic Poincaré disk. The distance between two nodes in the hyperbolic Poincaré disk is given by (34), which fairly complicates the conceptually easy computation. We content ourselves to refer to page 5 and Fig. 3 in Krioukov *et al.* [11] and only mention their result of the average degree of a node with radial coordinate r,

$$d_{av;HRHG}(r) \approx \frac{4}{\pi} N e^{-\frac{r}{2}} \tag{20}$$

The average degree in the entire network is computed from (20) as

$$d_{av;HRHG} = \int_0^R d_{av;HRHG}(x)\, g_{(r,\theta)}(x)\, dx \approx \frac{4N}{\pi} \int_0^R e^{-\frac{x}{2}} e^{x-R} dx = \frac{8N}{\pi} e^{-\frac{R}{2}}$$

which is an instance $E[D] = \int_0^R E[D|z] \frac{d\Pr[z \leq x]}{dx} dx$ of the law of total probability [5, p. 23], where $E[D|z] = d_{av;HRHG}(z)$ is the conditional expectation of the degree of a node, given its radial position $z = r$ in the the hyperbolic Poincaré disk. The resulting link density $p_{HRHG} = \frac{d_{av;HRHG}}{N-1}$ then follows approximately as

$$p_{HRHG} \approx \frac{8}{\pi} e^{-\frac{R}{2}} \tag{21}$$

The HRHG is a sparse graph, if we assume that the link density p_{HRHG} in (21) is low and the radius of R of the hyperbolic Poincaré disk is sufficiently large. For a sparse HRHG, assuming a Poisson degree distribution (see Section 3.2.1) is a reasonable approximation. The degree of a node at radial position $r = x$ then becomes

$$\Pr[D_{HRHG}(x) = k] = \frac{d_{av;HRHG}^k(x)}{k!} e^{-d_{av;HRHG}(x)} \tag{22}$$

The degree of an arbitrary node in HRHG follows from (22), again as an instance of the law of total probability [5, p. 23], as

$$\Pr[D_{HRHG} = k] = \int_0^R \Pr[D_{HRHG}(x) = k]\, g_{(r,\theta)}(x)\, dx \tag{23}$$

which is computed in Appendix B.1. Krioukov *et al.* [11] mention that

$$\Pr\left[D_{HRHG} = k\right] \approx ck^{-3}$$

which only holds for sufficiently large k and where c is constant (specified in Appendix B.1).

In summary, the degree D_{HRHG} of a random node in the Hard Random Hyperbolic Graph, whose particular construction and chosen parameters are outlined above, possesses a power law degree distribution (in the tail, i.e. for large k). Since many real-world network feature approximately such power law degree, a hyperbolic embedding "naturally" provides a power law-like degree distribution.

4.1 Comparison between HRRG (Euclidean) and HRHG (Hyperbolic)

In the Hard Random Geometric Graph (HRRG), N nodes are distributed uniformly over unit square (with size $Z = 1$) and linked if their Euclidean distance is below a connection radius r_0. The average degree in (12) is $d_{av;HRGG} = (N-1)\, p_{\square;HRGG}(r_0)$, where the link density is specified in (14) and (15) for any connection radius $r_0 \in [0, \sqrt{2}]$.

In the Hard Random Hyperbolic Graph (HRHG), computed by Krioukov *et al.* [11], nodes with polar coordinates (r, θ) are only uniformly at random distributed over all angular positions $\theta \in [0, 2\pi]$ for each radial position r. This choice then results in an average degree (20), depending on the distance r to the origin. The link density $p_{HRHG} = \frac{d_{av;HRHG}}{N-1}$, deduced from the average degree $d_{av;HRHG}$, is $p_{HRHG} \approx \frac{8}{\pi} e^{-\frac{R}{2}}$ in (21), which decreases exponentially with the radius R of the Poincaré hyperbolic disk. In contrast to a flexible connection radius r_0, Krioukov *et al.* [11] choose $r_0 = R$, which is very large compared to its Euclidean counter part.

Assuming that the Poisson approximation (Section 3.2.1) holds – Fig. 1 shows validity only for very small connection radius r_0 in HRGG – and that a certain given average degree d_{av} in both graph types is required, then the connection radius r_0 in (18) for the RGG scales, for large number N of nodes, as

$$r_0 \approx \sqrt{\frac{1}{\pi} \frac{d_{av}}{N}} \sim N^{-\frac{1}{2}}$$

For the HRHG, on the other hand, the link density (21) in HRHG leads to

$$r_0 = R \approx 2 \ln\left(\frac{8N}{\pi d_{av}}\right) \sim \log N$$

The scaling in connection radius r_0 in both types of random graphs is hugely different!

Acknowledgement

I am grateful to Roberto Gheda, Federico Ravazzolo, Robert Jankowski, Sámuel Balogh Gáspár and TU Delft students for instructive comments. Federico Ravazzolo has written Appendix C. I am supported by the European Research Council (ERC) under the European Union's Horizon 2020 research and innovation programme (grant agreement No 101019718).

References

[1] B. Bollobás. *Random Graphs.* Cambridge University Press, Cambridge, 2nd edition, 2001.

[2] R. van der Hofstad. *Random Graphs and Complex Networks*, volume 1 of *Cambridge Series in Statistical and Probabilistic Mathematics*. Cambridge University Press, Cambridge, U.K., notes at www.win.tue/ rhofstad/notesrgcn2023.pdf edition, 2018.

[3] M. Raftopoulou, R. Litjens, and P. Van Mieghem. Fréchet distribution in geometric graphs for drone networks. *Physical Review E*, 106(2):024301, 2022.

[4] P. Van Mieghem. Paths in the simple random graph and the Waxman graph. *Probability in the Engineering and Informational Sciences (PEIS)*, 15:535–555, 2001.

[5] P. Van Mieghem. *Performance Analysis of Complex Networks and Systems*. Cambridge University Press, Cambridge, U.K., 2014.

[6] E. C. Titchmarsh. *The Theory of Functions*. Oxford University Press, Amen House, London, 1964.

[7] P. Van Mieghem. *Graph Spectra for Complex Networks*. Cambridge University Press, Cambridge, U.K., 2nd edition, 2023.

[8] R. van der Hofstad, G. Hooghiemstra, and P. Van Mieghem. First passage percolation on the random graph. *Probability in the Engineering and Informational Sciences (PEIS)*, 15:225–237, 2001.

[9] Zhihao Q., S. G. Balogh, X. Liu, P. Van Mieghem, and M. Kitsak. Geometric organization and inference of shortest path nodes in soft random geometric graphs with Fermi-Dirac connection probability function. *Physical Review Research*, 8(3):033149, 2026.

[10] G. H. Hardy. *A Course of Pure Mathematics*. Cambridge University Press, 10th edition, 2006.

[11] D. Krioukov, F. Papadopoulos, M. Kitsak, A. Vahdat, and M. Boguña. Hyperbolic geometry of complex networks. *Physical Review E*, 82(3):036106, 2010.

[12] G. Sansone and J. Gerretsen. *Lectures on the Theory of Functions of a Complex Variable*, volume 1 and 2. P. Noordhoff, Groningen, 1960.

[13] T. L. Heath. *The Thirteen Books of EuclidÕs Elements*, volume I. Cambridge University Press, Cambridge, U. K., 2nd edition, 1926.

[14] E. T. Bell. *Men of Mathematics. The Lives and Achievements of the Great Mathematicians from Zeno to Poincaré*. A Touchstone Book, by Simon & Schuster, New York, 1937.

[15] P. Van Mieghem. *The Mittag-Leffler and Gamma function*. Oxford Mathematical Monographs. Oxford University Press, 2026.

[16] J. Dall and M. Christensen. Random geometric graphs. *Physical Review E*, 66:016121, 2002.

A Absolute geometry

Absolute geometry [12, Vol. II, Chapter 9] treats the three main geometries, Euclidean, Elliptic and Hyperbolic, as one framework in the curvature K as illustrated in Section A.5 below. If the curvature $K = 0$, then Euclidean geometry is obtained, while for curvature $K = 1$, absolute geometry reduces to Elliptic geometry and a curvature $K = -1$ generates Hyperbolic geometry.

The separation into three geometries is a consequence of the famous postulate 5 in Book 1 of Euclid [13, p. 155]:

Καi εαν εις δυο ευθειας ευθεια εμπiπτουσα τας εντος και επι τα αυτα μερη γωνιας δυο ορθων ελασσονας ποιη, εκβαλλομενας τας δυο ευθειας επ′ απειρον συμπιπτειν, εφ′ α μερη εισιν αι των δυο ορθων ελασσονες

That, if a straight line falling on two straight lines make the interior angles on the same side less than two right angles, the two straight lines, if produced indefinitely, meet on that side on which are the angels less than the two right angles.

Heath [13, p. 202-220] extensively explains Euclid's postulate 5 and discusses the views of a broad number of scholars before him that have interpreted (and tried to prove) postulate 5 and its consequences. Euclid's postulate 5 is alternatively known as [13, p. 220 (1)]

Through a given point only one parallel can be drawn to a given straight line.

The separation into three geometries started with a letter of the genius Carl Friedrich Gauss, Prince of Mathematics [14, Chapter 14], to his friend W. Bolay in 1799: "If I could prove that a rectilineal triangle is possible, the content of which is greater than any given area, I am in a position to prove perfectly rigorously the whole of geometry". Hence, it was Gauss who first expressed a conviction that the Postulate 5 could never be proved (see more historical sources in [13, p. 219]). Gauss did not publish anything about non-Euclidean geometry. Later, the published work of J. Bolay (son of W. Bolay) and Lobachevsky, independently, gave rise to non-Euclidean (i.e. both elliptic and hyperbolic) geometry.

In the sequel, we briefly explain Elliptic and Hyperbolic geometry, inspired by Sansone and Gerritsen [12].

A.1 Stereographic projection

Sansone and Gerritsen [12, p. 3-4] consider a unit sphere with center at the origin of the three-dimensional Cartesian coordinate axes (Fig. 2). On the surface of the sphere lies a point M' with coordinates (ξ, η, ζ). The south pole P, also on the unit sphere, has coordinates $(0, 0, -1)$. The stereographic projection of the M' on to the (two-dimensional) x, y-plane through the origin is the point M with coordinates $(x, y, 0)$. The points M', M and P lie on one line, called "collinear", so that they satisfy[12]

$$\frac{x}{\xi} = \frac{y}{\eta} = \frac{1}{1+\zeta}$$

whence,

$$x = \frac{\xi}{1+\zeta} \text{ and } y = \frac{\eta}{1+\zeta}$$

The converse, i.e. expressing (ξ, η, ζ) in terms of (x, y) relies on the equation of the unit sphere $\xi^2 + \eta^2 + \zeta^2 = 1$, as the surface where all points lie at equal distance $R = 1$ to the center.

A.2 Sphere and hyperboloid

The equation of a sphere $\xi^2 + \eta^2 + \zeta^2 = R^2$, centered at the origin with radius R, is rewritten as

$$\zeta = \pm\sqrt{R^2 - \xi^2 - \eta^2}$$

[12] If three points $a = (x_a, y_a, z_a), b = (x_b, y_b, z_b)$ and $c = (x_c, y_c, z_c)$ lie on one line, then in the coordinate axis with center the point, say c, the vectors $(x_a - x_c, y_a - y_c, z_a - z_c)$ and $(x_b - x_c, y_b - y_c, z_b - z_c)$ are parallel, which means that all their coordinates are proportional to some non-zero number k,

$$x_a - x_c = k\,(x_b - x_c)$$
$$y_a - y_c = k\,(y_b - y_c)$$
$$z_a - z_c = k\,(z_b - z_c)$$

Hence, collinearity means that

$$\frac{x_a - x_c}{x_b - x_c} = \frac{y_a - y_c}{y_b - y_c} = \frac{z_a - z_c}{z_b - z_c} = k$$

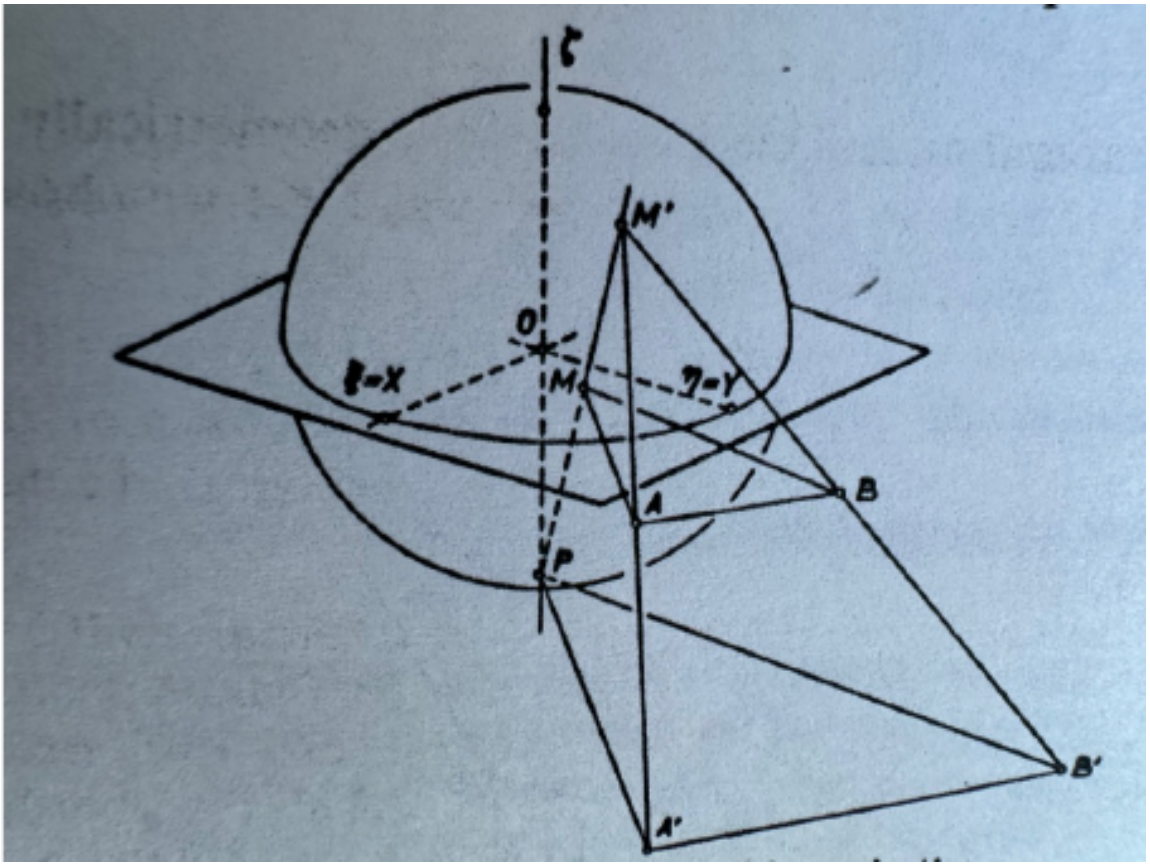


Figure 2: Stereographic projection from a point M' on the unit sphere to a point M in the x,y-plane. (Fig. copied from Sansone and Gerritsen [12, Fig. 1.1-4])

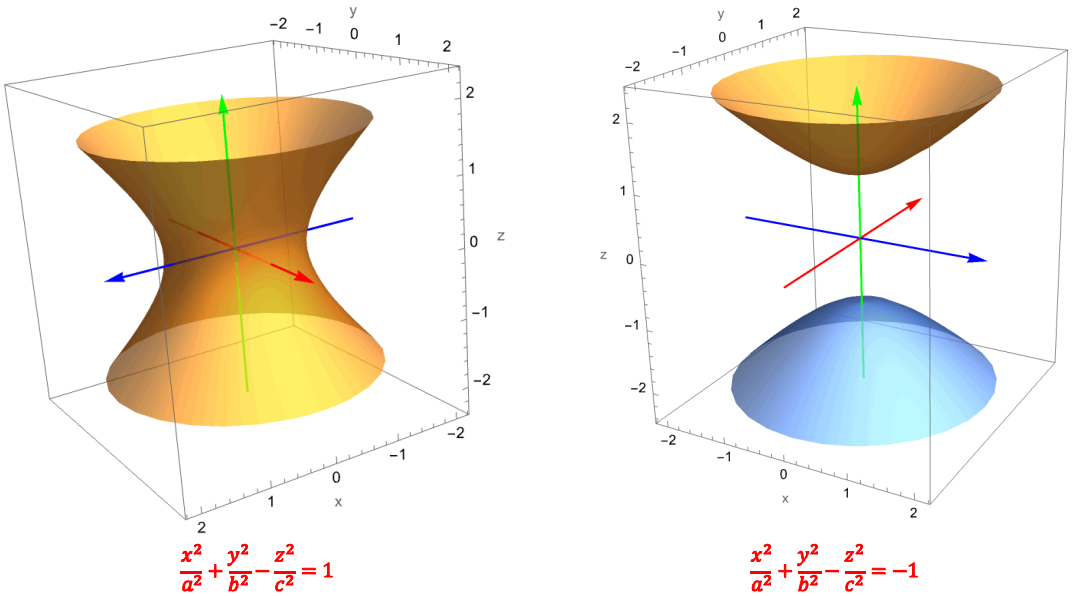


Figure 3: The one-sheet hyperboloid (left) has negative Gaussian curvature $K(x,y,z) = -\frac{c^6}{(c^4+(a^2+c^2)z^2)^2}$. The two-sheet hyperboloid (right) has positive Gaussian curvature $K(x,y,z) = \frac{c^6}{(c^4-(a^2+c^2)z^2)^2}$.

If $\eta^2+\zeta^2 > R^2$, then ζ becomes purely imaginary, which implies that such a sphere does not exist. However, the left-hand side exists, $\pm\sqrt{\xi^2+\eta^2-R^2} = i\zeta$ and tells that $i\zeta$ is real and $(i\zeta)^2 = -\zeta^2$. The corresponding equation

$$\xi^2+\eta^2-\zeta^2 = R^2$$

describes a one-sheet or hyperbolic hyperboloid[13]. The companion $\xi^2+\eta^2-\zeta^2 = -R^2$ is the two-sheet hyperboloid as illustrated in Fig. 3, with two separate surfaces, with positive ζ and negative ζ, mirrored with respect to the origin.

Since

$$\zeta^2 = \left(\sqrt{\xi^2+\eta^2}-R\right)\left(\sqrt{\xi^2+\eta^2}+R\right)$$

the hyperboloid has circles at constant ζ. Moreover, if ξ and η are large compared to R, the hyperboloid approaches his asymptotic form $\xi^2+\eta^2-\zeta^2 = 0$, which is a cone with top at the origin (0,0,0). Fig. 4 illustrates that the stereograph projection of a point H on the two-sheet hyperboloid into the Poincaré disk, a circle with finite radius, is entirely different than the stereograph projection of a point M' on the sphere, which covers the entire x,y-plane. Only the south pole at $(0,0,-1)$, that lies on the surface of the sphere, is projected to the point at infinity. The south pole $(0,0,-1)$ does not necessarily lie on the surface of the hyperboloid and merely serves as the third collinear point to define the stereographic projection.

[13] See e.g. https://mathworld.wolfram.com/One-SheetedHyperboloid.html.

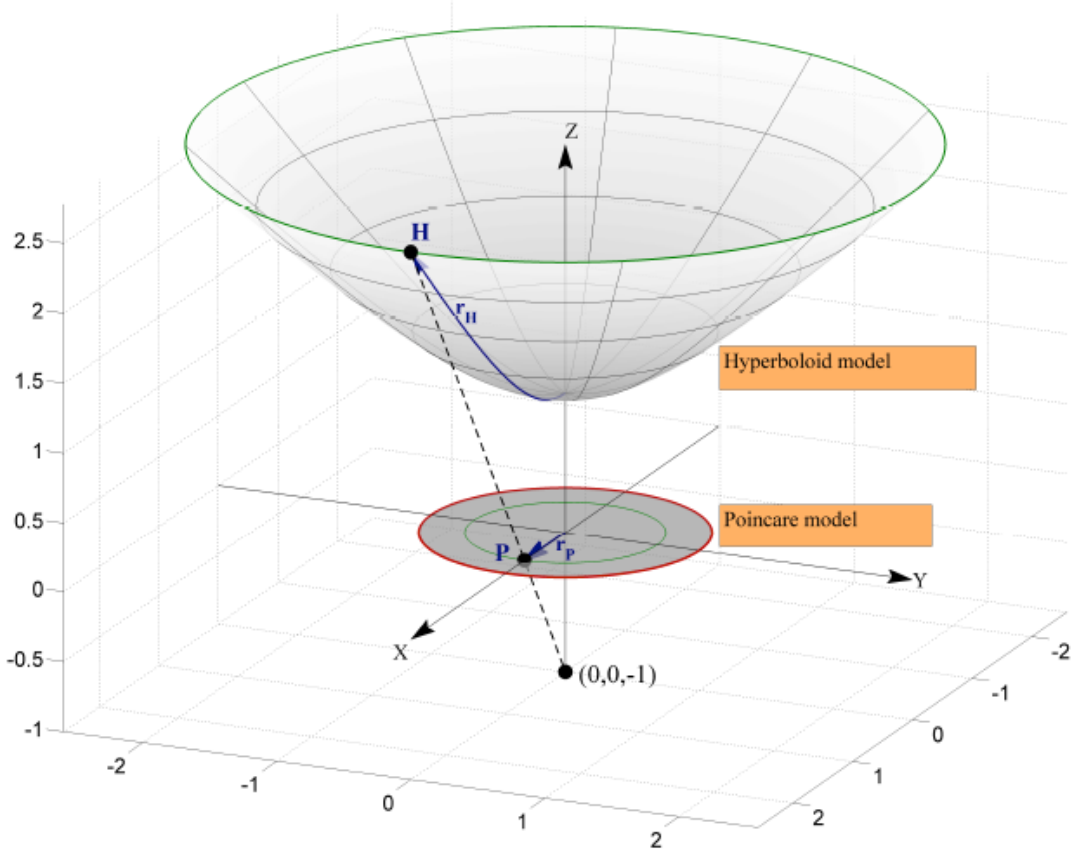


Figure 4: Stereographic projection from a point H' on the positive (i.e. $\zeta > 0$) hyperboloid to a point P in the Pioncaré disk, with the south pole at $(0, 0, -1)$ as in the sphere. (Fig. received from Maksim Kitsak)

A.3 Polar coordinates

Before proceeding, we add the representation of the a point on the sphere $\xi^2+\eta^2+\zeta^2=R^2$ in polar coordinates,

$$\begin{aligned}\xi &= R\cos\varphi\sin\theta\\ \eta &= R\sin\varphi\sin\theta\\ \zeta &= R\cos\theta\end{aligned}$$

The corresponding polar representation for a point on the one-sheet hyperboloid $\xi^2+\eta^2-\zeta^2=R^2$ is

$$\begin{aligned}\xi &= R\cos\varphi\cosh\theta\\ \eta &= R\sin\varphi\cosh\theta\\ \zeta &= R\sinh\theta\end{aligned}$$

A point on the two-sheet hyperboloid $\xi^2+\eta^2-\zeta^2=-R^2$ has polar coordinates

$$\begin{aligned}\xi &= R\cos\varphi\sinh\theta\\ \eta &= R\sin\varphi\sinh\theta\\ \zeta &= R\cosh\theta\end{aligned}$$

The stereographic projection of the M' on the sphere is the point M in the x,y-plane, which can be written as a complex number

$$z=x+iy=\frac{\xi+i\eta}{1+\zeta}$$

where the real axis $x=\mathrm{Re}\,(z)$ and the imaginary axis is $y=\mathrm{Im}\,(z)$. In polar coordinates,

$$\begin{aligned}z=\frac{\xi+i\eta}{1+\zeta}&=\frac{R\cos\varphi\sin\theta+iR\cos\varphi\sin\theta}{1+R\cos\theta}=\frac{R\sin\theta}{1+R\cos\theta}e^{i\varphi}\\ &=\frac{2R\sin\frac{\theta}{2}\cos\frac{\theta}{2}}{1-R+2R\cos^2\frac{\theta}{2}}e^{i\varphi}\overset{R=1}{=}\tan\frac{\theta}{2}e^{i\varphi}\end{aligned}\tag{24}$$

A.4 Elliptic plane

An infinitesimal line segment on the sphere satisfies

$$(ds)^2=(d\xi)^2+(d\eta)^2+(d\zeta)^2$$

which is the square infinitesimal distance between two points that lie infinitesimally close to each other on the sphere (by Pythogoras' theorem). Introducing the polar coordinates with $d\xi=-R\sin\theta\sin\varphi d\varphi+R\cos\varphi\cos\theta d\theta$ and similar for η and ζ coordinates, we find[14] that

$$(ds)^2=R^2\left(\sin^2\theta\,(d\varphi)^2+(d\theta)^2\right)\tag{25}$$

[14] Explicitly,

$$\begin{aligned}(ds)^2&=(-R\sin\theta\sin\varphi d\varphi+R\cos\varphi\cos\theta d\theta)^2+(R\sin\theta\cos\varphi d\varphi+R\sin\varphi\cos\theta d\theta)^2+R^2\sin^2\theta\,(d\theta)^2\\ &=R^2\sin^2\theta\sin^2\varphi\,(d\varphi)^2+R^2\cos^2\varphi\cos^2\theta\,(d\theta)^2-2R^2\sin\theta\sin\varphi\cos\varphi\cos\theta d\varphi d\theta\\ &+R^2\sin^2\theta\cos^2\varphi\,(d\varphi)^2+R^2\sin^2\varphi\cos^2\theta\,(d\theta)^2-2R^2\sin\theta\cos\varphi\sin\varphi\cos\theta d\varphi d\theta+R^2\sin^2\theta\,(d\theta)^2\\ &=R^2\sin^2\theta\,(d\varphi)^2+R^2\cos^2\theta\,(d\theta)^2+R^2\sin^2\theta\,(d\theta)^2\end{aligned}$$

Similarly, we deduce from (24), for $R = 1$, that

$$dz = i \tan \frac{\theta}{2} e^{i\varphi} d\varphi + \frac{1}{2} e^{i\varphi} \sec^2 \frac{\theta}{2} d\theta$$

from which, where $z^* = x - iy$ denotes the complex conjugate of $z = x + iy$,

$$\begin{aligned} |dz|^2 = dz\,(dz)^* &= \tan^2 \frac{\theta}{2} (d\varphi)^2 + \frac{1}{4} \sec^4 \frac{\theta}{2} (d\theta)^2 \\ &= \sin^2 \frac{\theta}{2} \sec^2 \frac{\theta}{2} (d\varphi)^2 + \frac{1}{4} \sec^4 \frac{\theta}{2} (d\theta)^2 \\ &= \frac{1}{4} \sec^4 \frac{\theta}{2} \left(\sin^2 \theta\, (d\varphi)^2 + (d\theta)^2 \right) \end{aligned}$$

Further, $1 + z^* z = 1 + |z|^2 = 1 + \tan^2 \frac{\theta}{2} = \sec^2 \frac{\theta}{2}$, so that $\left(1 + |z|^2\right)^2 = \sec^4 \frac{\theta}{2}$ and, with (25), we have

$$\frac{4\,|dz|^2}{\left(1 + |z|^2\right)^2} = \sin^2 \theta\, (d\varphi)^2 + (d\theta)^2 = (ds)^2$$

Hence, for a point $z = re^{i\theta}$ in the complex plane or "elliptic plane", the infinitesimal line segment (after stereographic projection based on collinearity) is

$$(ds_{\mathcal{E}})^2 = \frac{4\,|dz|^2}{\left(1 + |z|^2\right)^2} = \frac{4\left((dr)^2 + r^2 (d\theta)^2\right)}{(1 + r^2)^2} \tag{26}$$

Relation (26) enables us to compute the distance $r_{\mathcal{E}}$ from point M with coordinates (x, y) and complex representation $z = x + iy = re^{i\theta}$ to the origin as

$$r_{\mathcal{E}} = \int_0^r ds_{\mathcal{E}} = \int_0^r \frac{2dr}{(1 + r^2)} = 2 \arctan r$$

hence

$$r = \tan \frac{r_{\mathcal{E}}}{2}$$

Relation $z = \tan \frac{\theta}{2} e^{i\varphi}$ in (24) for the unit sphere $R = 1$ indicates that $\theta = r_{\mathcal{E}}$. Substituting $r = \tan \frac{r_{\mathcal{E}}}{2}$ into (26) yields

$$(ds_{\mathcal{E}})^2 = (dr_{\mathcal{E}})^2 + \sin^2 r_{\mathcal{E}}\, (d\theta)^2$$

Finally, an infinitesimal surface element in the x, y-plane (or complex plane z) in polar coordinates is

$$dS_{\mathcal{E}} = dr_{\mathcal{E}}.\, ds_{\mathcal{E}}|_{r_{\mathcal{E}} = \text{constant}} = \sin r_{\mathcal{E}} dr_{\mathcal{E}} d\theta$$

A.5 Absolute geometry

Sansone and Gerritsen [12, Section 9.5] treat hyperbolic geometry, based on automorphisms of the unit circle and Mobius transforms, and showed, after a considerably more involved analysis, that the infinitesimal line segment in the Poincaré disk or "hyperbolic plane", is

$$(ds_{\mathcal{H}})^2 = \frac{4\left((dr)^2 + r^2 (d\theta)^2\right)}{(1 - r^2)^2} \tag{27}$$

The striking similarity between (26) and (27) suggests to define absolute geometry by the infinitesimal line segment,

$$(ds_{\mathcal{A}})^2 = \frac{4\left((dr)^2 + r^2\,(d\theta)^2\right)}{(1+Kr^2)^2} \tag{28}$$

where K is the curvature of the surface. For example, $K = \frac{1}{R^2}$ is the Gaussian curvature of the sphere with radius R. All geometries with $K < 0$ and $K > 0$ do not differ essentially, which leads to three distinct classes: $K = 0$, for Euclidean geometry, $K > 0$ specifies elliptic geometry and $K < 0$ hyperbolic geometry. The distance $r_{\mathcal{A}}$ of a point z in the plane to the origin is

$$r_{\mathcal{A}} = \int_0^r ds_{\mathcal{A}} = \int_0^r \frac{2dr}{(1+Kr^2)} = \frac{2}{\sqrt{K}} \arctan\left(2\sqrt{K}\right)$$

The alternative infinitesimal line segment (similar as in Section A.4) is

$$(ds_{\mathcal{A}})^2 = (dr_{\mathcal{A}})^2 + \frac{1}{K}\sin^2\left(r_{\mathcal{A}}\sqrt{K}\right)(d\theta)^2 \tag{29}$$

while the corresponding infinitesimal surface element is

$$dS_{\mathcal{A}} = \frac{1}{\sqrt{K}}\sin\left(r_{\mathcal{A}}\sqrt{K}\right) dr_{\mathcal{A}} d\theta \tag{30}$$

We verify[15] for Euclidean geometry ($K \to 0$), that (30) reduces to the well-known differential for the area S in polar coordinates

$$dS = r dr d\theta$$

For hyperbolic geometry ($K < 0$), the infinitesimal line segment for a point $(r_{\mathcal{H}}, \theta_{\mathcal{H}})$ in the hyperbolic (Poincaré) disk follows from (29), with $K = -\,|K| < 0$ and

$$\begin{aligned}\sin^2\left(r_{\mathcal{H}}\sqrt{K}\right) &= \left(\sin\left(r_{\mathcal{H}}\sqrt{-\,|K|}\right)\right)^2 = \left(\sin\left(ir_{\mathcal{H}}\sqrt{|K|}\right)\right)^2 \\ &= \left(i\sinh\left(ir_{\mathcal{H}}\sqrt{|K|}\right)\right)^2 = -\sinh^2\left(r_{\mathcal{H}}\sqrt{|K|}\right)\end{aligned}$$

as

$$(ds_{\mathcal{H}})^2 = (dr_{\mathcal{H}})^2 + \frac{1}{|K|}\sinh^2\left(r_{\mathcal{H}}\sqrt{|K|}\right)(d\theta)^2$$

Similarly, the infinitesimal surface element (30) becomes

$$dS_{\mathcal{H}} = \frac{1}{\sqrt{|K|}}\sinh\left(r_{\mathcal{H}}\sqrt{|K|}\right) dr_{\mathcal{H}} d\theta \tag{31}$$

The length or perimeter of a circle with radius r in the the hyperbolic (Poincaré) disk is

$$L_{\text{circle}} = \int_0^{2\pi} ds_{\mathcal{H}}|_{r_{\mathcal{H}}=\text{ constant}} = \int_0^{2\pi} \frac{1}{\sqrt{|K|}}\sinh\left(r\sqrt{|K|}\right) d\theta$$

and

$$L_{\text{circle}} = \frac{2\pi}{\sqrt{|K|}}\sinh\left(r\sqrt{|K|}\right) \tag{32}$$

[15] Either apply de l'Hospital's limit rule $\lim_{y\to 0}\frac{f(y)}{g(y)} = \frac{0}{0} = \lim_{y\to 0}\frac{f'(y)}{g'(y)}$ or invoke the Taylor series $\sin z = \sum_{k=0}^{\infty}\frac{(-1)^k z^{2k+1}}{(2k+1)!}$ around $z_0 = 0$, which is convergent for all complex z. For small z, it holds that $\sin z = z + O\left(z^3\right)$.

while its area equals

$$A_{\text{circle}} = \int_0^{2\pi} \int_0^r dS_{\mathcal{H}} = \int_0^{2\pi} \int_0^r \frac{1}{\sqrt{|K|}} \sinh\left(u\sqrt{|K|}\right) du d\theta$$
$$= \frac{2\pi}{|K|} \cosh\left(u\sqrt{|K|}\right)\Big|_{u=0}^{u=r}$$

resulting in

$$A_{\text{circle}} = \frac{2\pi}{|K|}\left(\cosh\left(r\sqrt{|K|}\right) - 1\right) \tag{33}$$

If the curvature tends to zero, $K \to 0$, then the area A_{circle} in (33) reduces, after twice applying de l'Hospital's rule or after introducing the Taylor expansion of $\cosh(x) = \sum_{k=0}^{\infty} \frac{x^{2k}}{(2k)!} = 1 + \frac{x^2}{2} + O\left(x^4\right)$, to the well-known Euclidean circular area $A_{\text{circle},} = \pi r^2$.

The distance $d(z_1, z_2)$ between two points z_1 and z_2 with polar coordinates (r_1, θ_1) and (r_2, θ_2), respectively, in the hyperbolic Poincaré disk is specified by the "hyperbolic law of cosines"

$$\cosh\left(d(z_1, z_2)\sqrt{|K|}\right) = \cosh\left(r_1\sqrt{|K|}\right)\cosh\left(r_2\sqrt{|K|}\right) - \sinh\left(r_1\sqrt{|K|}\right)\sinh\left(r_2\sqrt{|K|}\right)\cos\left(\|\theta_1 - \theta_2\|\right) \tag{34}$$

where $\|\theta_1 - \theta_2\| = \pi - |\pi - |\theta_1 - \theta_2||$ is the angle between the points z_1 and z_2. The proof of (34), which can be deduced from (29), is involved and omitted.

Sansone and Gerritsen [12, Section 9.6.3] prove (via Euler equations in variational calculus that characterize the shortest distance curves, i.e. the geodesics) that the area Δ of a triangle with angles α, β and γ in absolute geometry is

$$K\Delta = \alpha + \beta + \gamma - \pi \tag{35}$$

Apart from Euclidean geometry ($K = 0$), the area Δ of a triangle in absolute geometry is entirely determined by its three angles α, β and γ. Formula (35) demonstrates the famous result that in elliptic geometry ($K > 0$), the sum $\alpha+\beta+\gamma$ of the angles of a triangle is larger than π, in hyperbolic geometry ($K < 0$), the sum of the angles of a triangle is smaller than π, while perfectly equal to π in Euclidean geometry ($K = 0$).

B Computations

B.1 Approximate power law deep tail approximation for degree in HRHG

We compute the probability of the degree in HRHG from (23),

$$\Pr\left[D_{HRHG} = k\right] = \int_0^R \Pr\left[D_{HRHG}(x) = k\right] g_{(r,\theta)}(x)\, dx$$

We insert the Poisson approximation (22) of the degree,

$$\Pr\left[D_{HRHG} = k\right] \approx \frac{1}{k!} \int_0^R d_{av;HRHG}^k(x)\, e^{-d_{av;HRHG}(x)} e^{x-R} dx$$

and introduce the estimate $d_{av;HRHG}(r) \approx \frac{4}{\pi} N e^{-\frac{r}{2}}$ in (20) for the average degree at a radial position x,

$$\begin{aligned}\Pr[D_{HRHG} = k] &\approx \frac{1}{k!} \int_0^R d_{av;HRHG}^k(x)\, e^{-d_{av;HRHG}(x)} e^{x-R} dx \\ &= \frac{\left(\frac{4}{\pi}N\right)^k e^{-R}}{k!} \int_0^R e^{-\frac{kx}{2}} e^{-\frac{4}{\pi}Ne^{-\frac{x}{2}}} e^x dx = \frac{\left(\frac{4}{\pi}N\right)^k e^{-R}}{k!} \int_0^R e^{-\left(\frac{k}{2}-1\right)x} e^{-\frac{4}{\pi}Ne^{-\frac{x}{2}}} dx\end{aligned}$$

Let $u = \frac{4}{\pi} N e^{-\frac{x}{2}}$, then $x = -2\log\left(\frac{\pi}{4N}u\right)$ and $dx = -\frac{2}{u}du$,

$$\begin{aligned}\int_0^R \left(e^{-\frac{x}{2}}\right)^{(k-2)} e^{-\frac{4}{\pi}Ne^{-\frac{x}{2}}} dx &= 2\int_{\frac{4}{\pi}Ne^{-\frac{R}{2}}}^{\frac{4}{\pi}N} \left(\frac{\pi}{4N}u\right)^{(k-2)} e^{-u}\frac{du}{u} = 2\left(\frac{\pi}{4N}\right)^{(k-2)} \int_{\frac{4}{\pi}Ne^{-\frac{R}{2}}}^{\frac{4}{\pi}N} u^{(k-2)-1} e^{-u} du \\ &\simeq 2\left(\frac{\pi}{4N}\right)^{(k-2)} \int_{\frac{d_{av;HRHG}}{2}}^{\infty} u^{(k-2)-1} e^{-u} du\end{aligned}$$

In terms of the incomplete Gamma function $\Gamma(a,z) = \int_z^\infty u^{a-1}e^{-u}du$ in [15, Eq. (16.1) on p. 283] and with $\Gamma(k+1) = k!$, we obtain approximately

$$\Pr[D_{HRHG} = k] \approx 2\left(\frac{d_{av;HRHG}}{2}\right)^2 \frac{\Gamma\left(k-2, \frac{d_{av;HRHG}}{2}\right)}{\Gamma(k+1)}$$

For sufficiently small $d_{av;HRHG}$, we approximate $\Gamma\left(k-2, \frac{d_{av;HRHG}}{2}\right) \approx \Gamma(k-2,0) = \Gamma(k-2)$ and use the functional equation $\Gamma(z+1) = z\Gamma(z)$ in [15, (10.1) on p. 181] of the Gamma function, resulting in

$$\frac{\Gamma\left(k-2, \frac{d_{av;HRHG}}{2}\right)}{\Gamma(k+1)} \approx \frac{\Gamma(k-2)}{\Gamma(k+1)} = \frac{\Gamma(k-2)}{k(k-1)(k-2)\Gamma(k-2)} = \frac{1}{k(k-1)(k-2)}$$

Finally, for sufficiently large k, we arrive approximately at the deep tail probability (thus only for large k)

$$\Pr[D_{HRHG} = k] \approx 2\left(\frac{d_{av;HRHG}}{2}\right)^2 k^{-3}$$

C Clustering coefficient of a Hard Random Geometric Graph on 2D torus

We consider a Hard Random Geometric Graph (HRGG) with N nodes, placed independently and uniformly at random in a square with size Z. Node i at position r_i and node j at position r_j are connected by a link if their distance $|r_i - r_j|$ is smaller than the connection radius r_0, i.e. the link connection function is $f(r) = 1_{\{r \le r_0\}}$. The link density of a 2D HRGG on a square, illustrated in Figure 5 (right) is computed in Section 3.1. Following Dall and Christensen [16], we impose periodic boundary conditions: opposite sides of the square are folded and nodes close the upper (or left) boundary can connect to nodes close to the lower (or right) boundary of the square, so that the square becomes a torus $\mathbb{T}$ in 3D and the distance $|r_i - r_j|$ is measured along the shortest path on the torus (Figure 5, left). The boundary effects that complicate the link density (14) and (15) disappear. The

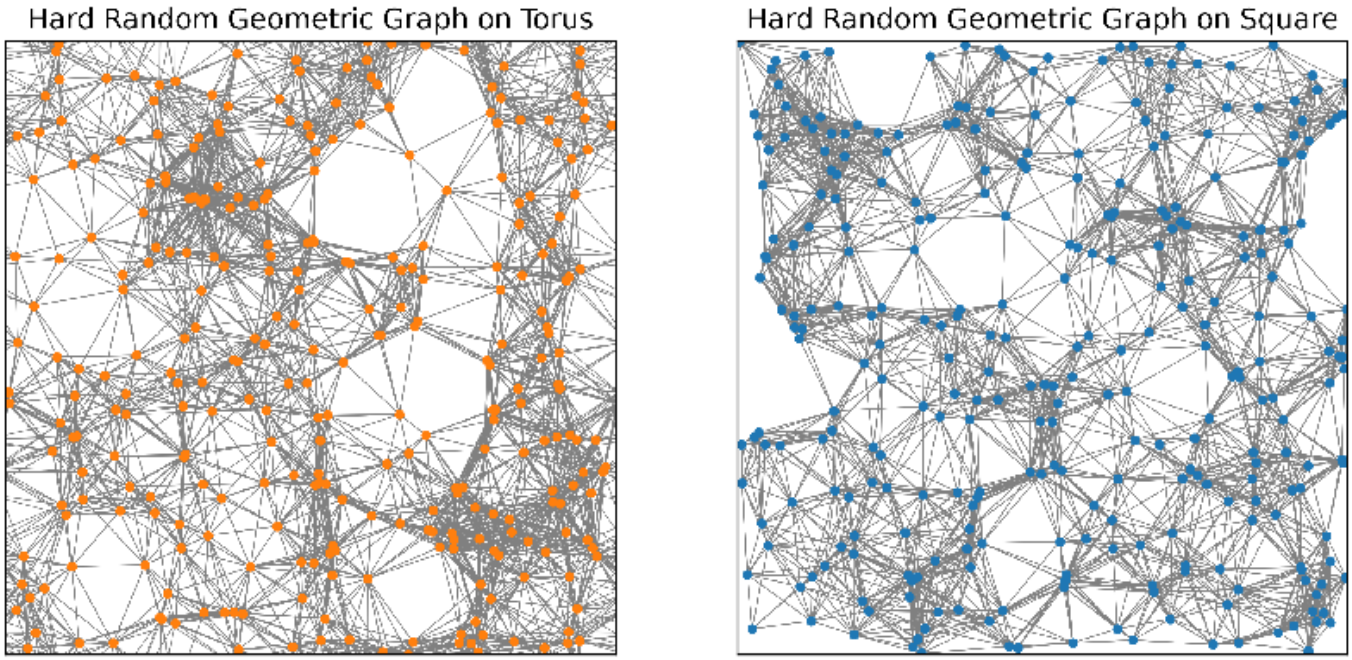


Figure 5: HRGG with $N = 300$ nodes and connection radius $r_0 = 0.15$ with discrete (right) and continuous boundary conditions (left).

circle $C_i(r_0)$ with center at node i, radius r_0 and surface area $S[C_i(r_0)]$ lies entirely within the torus if $r_0 \leq Z/2$, and the link density (11) becomes exactly,

$$p_{\mathbb{T};HRGG}(r_0) = \Pr\left[\mathcal{D} \leq r_0\right] = \frac{S\left[C_i(r_0)\right]}{Z^2} = \pi \left(\frac{r_0}{Z}\right)^2 \tag{36}$$

which equals the Poisson approximation (17) of the square.

The graph clustering coefficient c_G is the ratio of the number of labelled triangles and the number of labelled connected triples [5, Sec. 15.6.5],

$$c_G = \frac{\sum_{k=1}^{N} \sum_{i \in \mathcal{N}_k} \sum_{j \in \mathcal{N}_k \setminus \{i\}} a_{ij}}{\sum_{k=1}^{N} d_k(d_k - 1)} \tag{37}$$

where $\mathcal{N}_k$ is the set of neighbors of node k, $d_k = |\mathcal{N}_k|$ is the degree of node k and a_{ij} is the element of the adjacency matrix A. Replacing the numerator and denominator in (37) by their expectation and using that all ordered triples (k, i, j) are statistically equivalent, gives the clustering coefficient $c_{\mathbb{T};HRGG}$ of the HRGG on the torus,

$$c_{\mathbb{T};HRGG} = \frac{\Pr\left[a_{ij} = 1, a_{ik} = 1, a_{jk} = 1\right]}{\Pr\left[a_{ik} = 1, a_{jk} = 1\right]} = \Pr\left[a_{ij} = 1 \middle| \; a_{ik} = 1, a_{jk} = 1\right] \tag{38}$$

i.e. the clustering coefficient is the probability that two neighbors i and j of a node k are linked. For large N, the graph clustering coefficient c_G of a single realization concentrates around the expected clustering coefficient (38). In terms of the circles with radius r_0, the clustering coefficient in (38) reads

$$c_{\mathbb{T};HRGG} = \Pr\left[j \in C_i(r_0) \middle| \; i \in C_k(r_0),\, j \in C_k(r_0)\right]$$

Node j is uniformly distributed over the circle $C_k(r_0)$, independently of node i. Hence, for a given position of node i, the probability that $j \in C_i(r_0)$ equals the fraction of the area of $C_k(r_0)$ that overlaps with $C_i(r_0)$,

$$c_{\mathbb{T};HRGG} = E\left[\frac{S\left[C_i(r_0) \cap C_k(r_0)\right]}{S\left[C_k(r_0)\right]}\right] \tag{39}$$

The overlapping area $S[C_i(r_0) \cap C_k(r_0)]$ is shaded in the diagram in Figure 6. Denote by $r = |r_i - r_k|$

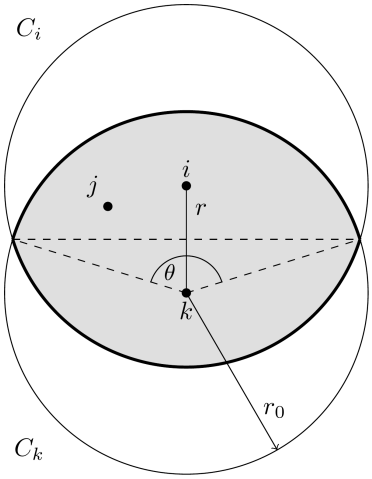


Figure 6: The circles $C_k(r_0)$ and $C_i(r_0)$ with radius r_0 around node k and node i at distance r. Node j is a common neighbor of k and i if node j lies in the shaded overlapping area $S[C_i(r_0) \cap C_k(r_0)]$, bounded by the thick lines.

the distance between nodes i and k, which varies from 0 to r_0. The overlapping area of two circles with radius r_0, whose centers lie at distance $r \leq 2r_0$, equals (cool problem for the reader):

$$S\left[C_i(r_0) \cap C_k(r_0)\right] = r_0^2\left(\theta - \sin\theta\right), \qquad \theta = 2\arccos\left(\frac{r}{2r_0}\right) \tag{40}$$

Since $S\left[C_k(r_0)\right] = \pi r_0^2$, the area ratio (39) becomes

$$\frac{S\left[C_i(r_0) \cap C_k(r_0)\right]}{S\left[C_k(r_0)\right]} = \frac{\theta - \sin\theta}{\pi}$$

which depends on node i only via the distance r. Given that $i \in C_k(r_0)$, node i is uniformly distributed over $C_k(r_0)$ and the probability density function of the distance r is $2r/r_0^2$ for $0 \leq r \leq r_0$. The expected area overlap gives the clustering coefficient:

$$c_{\mathbb{T};HRGG} = \int_0^{r_0} \frac{S\left[C_i(r_0) \cap C_k(r_0)\right]}{S\left[C_k(r_0)\right]} \frac{2r}{r_0^2} dr = \frac{2}{\pi}\int_{2\pi/3}^{\pi} (\theta - \sin\theta)\sin\theta d\theta = 1 - \frac{3\sqrt{3}}{4\pi} \approx 0.5865 \tag{41}$$

where the term $-2\sin\theta d\theta$ comes from the change of variable from r to θ in (40):

$$r^2 = 4r_0^2\cos^2\left(\frac{\theta}{2}\right) = 2r_0^2\left(1 + \cos(\theta)\right), \quad 2rdr = -2r_0^2\sin(\theta)d\theta$$

The clustering coefficient (41) of a HRGG on a torus does not depend on the number of nodes N, nor on the connection radius r_0, nor on the link density p in (36). Two important remarks: (i) Two

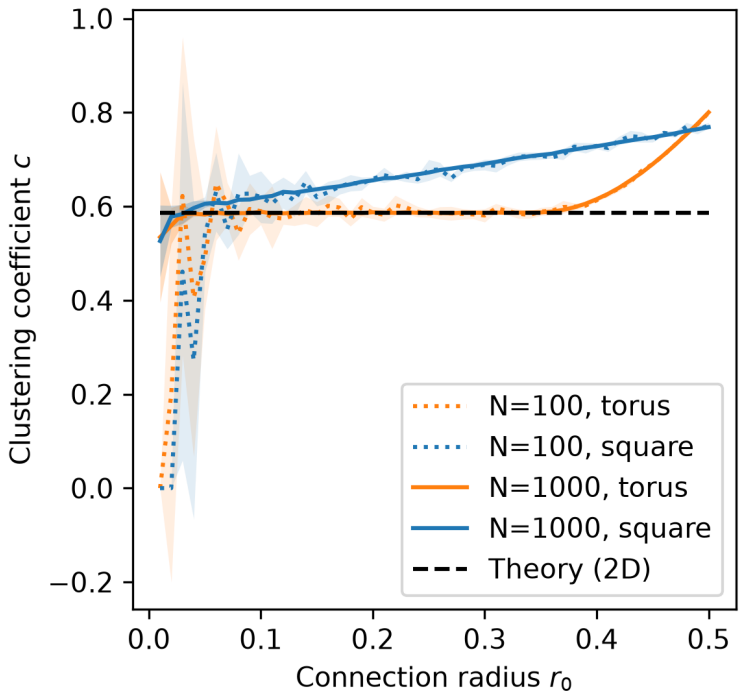


Figure 7: Average clustering coefficient (37) of 5 realizations of a HRGG with discrete (blue) and continuous (orange) boundary conditions, as a function of the connection radius r_0, compared with the theoretical expectation (41).

neighbours i and j of k, at most at distance $2r_0$, are connected by a path of length $Z - r_0$ around the torus of size Z, if $Z - 2r_0 < r_0$. Then, if the connection radius is larger than $r_0 > \frac{Z}{3}$, then (40) underestimates the overlapping area and (41) underestimates the clustering coefficient. (ii) Instead, when the connection radius and the number of nodes are small: (41) is the exact expectation, but fluctuations are high since there are few connected triples on average (Figure 7, bottom right).